

PSI: A Pedestrian Behavior Dataset for Socially Intelligent Autonomous Car

Tina Chen^{†*}, Taotao Jing^{‡*}, Renran Tian[†], Yaobin Chen[†], Joshua Domeyer[‡],
Heishiro Toyoda[‡], Rini Sherony[‡], Zhengming Ding[‡]

[†]Indiana University Purdue University-Indianapolis, [‡]Tulane University, [‡]Toyota Motor North America

Abstract—Prediction of pedestrian behavior is critical for fully autonomous vehicles to drive in busy city streets safely and efficiently. The future autonomous cars need to fit into mixed conditions with not only technical but also social capabilities. As more algorithms and datasets have been developed to predict pedestrian behaviors, these efforts lack the benchmark labels and the capability to estimate the temporal-dynamic intent changes of the pedestrians, provide explanations of the interaction scenes, and support algorithms with social intelligence. This paper proposes and shares another benchmark dataset called the *IUPUI-CSRC Pedestrian Situated Intent (PSI)* data with two innovative labels besides comprehensive computer vision labels. The first novel label is the *dynamic intent changes* for the pedestrians to cross in front of the ego-vehicle, achieved from 24 drivers with diverse backgrounds. The second one is the *text-based explanations* of the driver reasoning process when estimating pedestrian intents and predicting their behaviors during the interaction period. Consequently, we develop a novel Explainable Pedestrian Trajectory Prediction (eP2P) model conditioned on the pedestrian intent/behavior prediction and its corresponding explicit explanations. The PSI dataset can fundamentally improve the development of pedestrian behavior prediction models and develop socially intelligent autonomous cars to interact with pedestrians efficiently. The dataset has been evaluated with different tasks and released to the public http://situated-intent.net/pedestrian_dataset/.

Index Terms—Pedestrian Behavior Benchmark, Explainable Learning

I. INTRODUCTION

With the increased automation levels and advanced technologies, autonomous vehicles (AVs) can cruise safely in many highway and freeway situations. However, the complex scenes of mixed traffic in urban settings, especially with pedestrians, remain challenging and create AV-involved traffic conflicts [1]. Interactions with pedestrians not only are safety-critical but also affect traffic efficiency and user attitudes like trust and acceptance [2]. Facing pedestrians, the current path and motion planning algorithms make decisions based on their trajectories [3] and optimize the ego motions to avoid crashes [4]. In this process, vehicle dynamics are usually calculated based on motion parameters of all the involved objects [5] or learning-based models to predict the future trajectories and actions [3], [6]. There are increasing numbers of algorithms and benchmark datasets published in this domain in the past several years [7].

The performance of pedestrian behavior prediction algorithms, like trajectory prediction and action recognition, has achieved significant improvements. However, several fundamental limitations still obstruct smooth and efficient AV-pedestrian interactions. Driving is not only a technical skill but also a social skill [8], [9]. This perspective from social science emphasizes the importance of social factors like goals and intent of different road users and the role of personal experiences in understanding and planning behaviors during interactions. Similar to human drivers, AVs need to continuously coordinate with other human road users by exchanging intents [9].

Although pedestrian intent is not a new concept for pedestrian behavior prediction, **there are no clear and consistent definitions of pedestrian intent** in the current literature [10]. Most existing studies use trajectories, postures, and actions (e.g., walking) as surrogates of actual pedestrian intent. In [11], the authors define pedestrian intent as the desire to cross the street, and apply human subject experiments to estimate such pedestrian crossing desires. This work opens the door to study pedestrian intent from the driver’s perspective, but the defined crossing desire does not reflect the intent dynamics during the car/driver-pedestrian interaction process. Considering intent as the direct and prominent predictor of human actions [12], a better annotation of pedestrian intent is necessary that changes with the dynamic situations.

Many ethnological studies [13], [14] have noticed the negotiation activities and corresponding behavioral cues during vehicle-pedestrian interactions. However, **no existing benchmark dataset differentiates pedestrian behaviors in and out of the interaction phases**. During interactions, pedestrian behaviors are contingent on the dynamic situations, creating a wicked learning environment [15]. In such conditions, behavior patterns learned in prior experiences may not always apply into future cases, and many behavioral cues convey social signals in addition to achieving moving objectives. Such a situation is difficult for AI algorithms to directly map scenario features to actions and trajectories without understanding the changes of pedestrian intents behind.

One last limitation is that **the current pedestrian behavior prediction algorithms lack explainability and reasoning capability**. Explainability of autonomous driving has been emphasized in general to improve algorithm performance and user attitude [16]. Verbal explanations from human drivers are essential components in improving algorithm explainability [17]. However, no existing research has been applied or

* indicates the equal contribution, and Renran Tian is the corresponding author, e-mail: rtian@iupui.edu

benchmark data constructed for pedestrian behavior prediction following this direction. Considering the large number of behavioral and contextual cues affecting pedestrian behaviors [18], [19], more research needs to understand driver reasoning better and integrate human knowledge to support the learning of holistic features and improve AI reasoning capability [20], [21].

A. Our Contributions

The IUPUI-CSRC Pedestrian Situated Intent (PSI) dataset is developed to address the limitations mentioned above in the current pedestrian behavior research area. The PSI dataset aims to support the development of socially intelligent AVs that interact with pedestrians in a fundamentally different way through a novel view of pedestrian intentions. Based on the theory of planned behavior [12], [22], behavioral intention captures the motivational factors and indicates how hard people are willing to try to perform the behavior. Intention shall be seen from a hierarchical structure, including goals, plans, intents, and activities [23], and intention exchange is the core of non-verbal interactions among drivers and pedestrians to solve potential conflicts [24]. With the emphasis on pedestrian intention, this research highlights several unique contributions.

Firstly, this research proposes a new definition of pedestrian intent, namely Pedestrian Situated Intent, as the pedestrian’s intent to cross in front of the car during the interactions and under contextual situations. Based on the theory of situated action [25], pedestrians have higher-level plans to move to the destinations. However, the actual actions are in response to the road situations. From the AVs’ path planning perspectives, pedestrians’ actions to cross in front of the ego-car are the most critical behavior, and the corresponding behavioral intentions are vital to planning AVs’ social actions. The Pedestrian Situated Intent is a temporal-dynamic state of the pedestrian, which determines their motions and/or social behaviors while also being affected by the changes of the situations, including the driver’s behavior and other environmental circumstances.

Secondly, a benchmark dataset (PSI) focusing on Pedestrian Situated Intent is created and released. The PSI dataset provides annotations of Pedestrian Situated Intent changes for 110 representative pedestrian crossing cases, supported by text-based explanations about the driver’s understanding of the scenes and the reasoning process to estimate pedestrian intent. These intent estimations and explanations are collected from 24 human drivers/annotators for each scene and synchronized at Pedestrian Situated Intent segmentation boundaries. These annotators are from different age groups (19 to 77 years old) and balanced genders to improve data representativeness. At the same time, the PSI dataset contains comprehensive and accurate manual annotations of common visual labels, such as object detection (for road users and infrastructure), object categories, semantic segmentation, object tracking, and pedestrian postures. This rich visual feature space can support different computer vision tasks.

Finally, we develop a novel explainable Pedestrian Trajectory Prediction (**eP2P**) algorithm towards complex scenes, incorporating the novel annotations in the PSI dataset. In

particular, Pedestrian Situated Intent labels, corresponding human reasoning descriptions, and the disagreement levels among human annotations are integrated to equip the algorithm with more human cognitive features. As a result, a multi-task learning model is designed to predict pedestrian intent changes with explicit explanation as well as pedestrian trajectories from the visual video inputs. The eP2P algorithm has achieved improved accuracies compared with baseline and existing models. The capabilities to predict pedestrian intent changes, explain the reasoning process, and improve trajectory prediction accuracies all demonstrate the power of the novel dataset and algorithm towards better understanding and modeling of pedestrian crossing scenes.

B. Related datasets

Pedestrian Behavior Datasets. In the last few years, there has been a sharp increase in the number of datasets released for autonomous vehicle research. These datasets are typically collected in major urban environments. Newer datasets [31]–[35] tend to focus on using sensor fusion (LiDAR and radar) to generate 3D and topological scene recreations. The main tasks for these datasets are object detection and tracking, because fusion data allows for more accurate automatic annotations. Both Apolloscape [31] and A2D2 [33] also have semantic segmentation from the ego-view for scene parsing tasks. However, these multimodal datasets usually do not include additional data for predicting pedestrian behavior. Except for BDD-100K [30], the lower half of Table I compares datasets collected with fusion sensors.

The top half of Table I compares datasets that have more pedestrian-centric annotations. JAAD [26] is one of the earlier datasets that started annotating pedestrian actions to study their crossing behavior with scene attributes also heavily annotated. STIP [27] contains pedestrian crossing action annotations, but lack additional attributes other than tracked bounding boxes. TITAN [36] classifies pedestrian actions into 43 sub-categories to try to explain their behavior. PedX [29] focuses on 3D human pose annotations to explain pedestrian behavior. *PIE [11] and our dataset, PSI, are the only datasets that measure pedestrian crossing intention. Different from the dynamic intents in PSI, the PIE defines a static pedestrian road-crossing desire for each case.*

Explainable AV Datasets. For explainable AV datasets, normally there are both visual inputs and text annotations. Berkeley Deep Drive eXplanation (BDD-X) dataset [17] is a subset of the BDD dataset [37] with action description and justification for all the driving events along with their timestamps. BDD Object Induced Actions (BDD-OIA) dataset [38] is a subset of BDD100K [30] video clips containing at least 5 pedestrians or bicycle riders and more than 5 vehicles. To increase scene diversity, these videos were selected under various weather conditions and times of the day. This resulted in 22,924 5-second video clips, which were annotated on MTurk for the 4 actions and 21 explanations. *None of the existing datasets explains pedestrian crossing intents in naturalistic scenes.*

TABLE I

COMPARISON OF POPULAR AV RESEARCH DATASETS. THE TOP HALF ARE PEDESTRIAN BEHAVIOR DATASETS. THE BOTTOM HALF ARE MAJOR DATASETS THAT INCLUDE BUT DO NOT FOCUS ON PEDESTRIAN BEHAVIOR. *NUMBER OF ANNOTATED FRAMES ONLY INCLUDE 2D ANNOTATIONS.

[§]SEGMENTATION FROM THE EGO-VIEW. [†]NUMBER OF CLASSES USED FOR ANNOTATING OBJECTS IN THE DATASET. [‡]NUMBER OF FRAMES MANUALLY ANNOTATED. **DATASET CONTAINS LiDAR DATA BUT WE DO NOT CONSIDER IT IN THIS SUMMARY. ^{††}ONLY CONTAINS INSTANCE SEGMENTATION OF PEDESTRIANS. ^{†††}REFERS TO WAYMO OPEN MOTION DATASET.

Dataset	Year	#Frames*	B-Boxes	Pose	Segt [§]	Track	Class [†]	Int	Act	Rsn
Ours (PSI)	2021	25k	✓	✓	✓	✓	20	621k	✗	✓
JAAD [26]	2016	82k	✓	✗	✗	✓	3	✗	✓	✗
PIE [11]	2019	293k	✓	✗	✗	✓	6	27k	✓	✗
STIP [27]	2020	110k [‡]	✓	✗	✗	✓	1	✗	✓	✗
TITAN [28]	2020	75k	✓	✗	✗	✓	3	✗	✓	✗
PedX** [29]	2019	5k	✗	✓	✓ ^{††}	✓	1	✗	✗	✗
BDD-100K [30]	2018	100k	✓	✗	✓	✓	10	✗	✗	✗
Apolloscape** [31]	2018	144k	✓	✗	✓	✓	5	✗	✗	✗
nuScenes** [32]	2019	40k	✓	✗	✗	✓	23	✗	✗	✗
A2D2** [33]	2020	41k	✓	✗	✓	✓	38	✗	✗	✗
Argo** [34]	2019	22k	✓	✗	✗	✓	15	✗	✗	✗
Lyft L5**	2019	55k	✓	✗	✗	✓	3	✗	✗	✗
Waymo** ^{†††} [35]	2021	—	✓	✗	✗	✓	3	✗	✗	✗

II. THE PSI DATASET

A. Data Preparation

The PSI dataset contains 110 representative vehicle-pedestrian encounters that happened at mid-block road locations with potential conflicts. These cases were sampled from the TASI 110-car naturalistic driving study [36]. In the driving study, 110 drivers were recruited to install a data collection system in each of their own cars. For one whole year, the positions of and the driving scenes in front of the subject’s cars were continuously recorded whenever the subjects were driving. From 1.4 million miles of driving data in different scenes, a total of more than 70,000 pedestrian encounters were identified across all the 110 cars. Multiple data annotators manually checked all these encounters to identify potential conflict cases. The potential conflict is defined as that at a particular timestamp during the encounter, crashes would happen if both the car and the pedestrian keep their instantaneous speed and directions [36]. A total of more than 3,000 potential conflict encounters were labeled in the whole data set. From these 3,000 cases, 110 encounters in mid-block road locations were randomly selected for the PSI dataset. These cases have the following features: **a)** Each case is 15 second with scene videos at 30 fps, GPS coordinates at 1 fps, and vehicle speed at 1 fps; **b)** All the cases happened at mid-block with higher driving speeds and more dangerous interactions; **c)** Every case has potential conflicts from the human driver’s perspective, meaning that average human drivers feel that at a particular moment during the interaction, a crash with the pedestrian will happen if both the car and the pedestrian keep the instantaneous speeds and moving directions.

B. Overview of the PSI Dataset

There are two types of labels in PSI: visual and cognitive annotations.

Lower-Level Visual Annotations. This step includes bounding boxes, pedestrian pose estimation, and semantic segmentation. Bounding boxes and pose estimation are all tracking

enabled, so each object and pose estimation is tracked for the entirety of the video clip. We annotated 10 classes of traffic objects and agents for bounding boxes, and an additional 10 classes of background information for semantic segmentation.

For the 110 video clips in PSI, there are 25,881 frames annotated with lower-level annotations. In the dataset, there are 239,470 bounding box annotations for traffic objects and agents. In these 110 encountering scenes, 180 pedestrians have pose estimation annotated using the MS COCO [39] format for annotating human pose estimation. In PSI, there are 24,579 unique pose estimations for the 180 pedestrians. 110 pedestrians out of the 180 were identified as key pedestrians that also have cognitive annotations. Additionally, one key frame for each video is annotated for generating 110 frames with complete semantic segmentation.

Higher-level Cognitive Annotations. This part includes pedestrian situated intent segmentation and human reasoning descriptions for pedestrian intent estimation, as illustrated in Figure 1. **(a) Pedestrian Situated Intent Segmentation** is shown as polygonal chains representing the estimated pedestrian intents to cross in front of the ego-vehicle. The intentions can switch from three states, namely “Cross”, “Not Cross”, and “Not Sure”. Each polygonal curve is the time-based estimation from one human driver/annotator, classifying the pedestrian’s situated intent into one of the three categories every frame. The vertices form the boundaries of interaction event segmentation based on the pedestrian intent changes. **(b) Human Reasoning Descriptions** are collected as text explanations corresponding to all the vertices along all the pedestrian intent segmentation polygonal curves. These descriptions explain the most critical reasoning logic from human drivers/annotators to judge the Pedestrian Situated Intents during the preceding scene segments.

Annotator Statistics: 24 data annotators were recruited in this study. Each annotator labels all the 110 encountering scene videos through a video experiment to obtain these labels. All the annotators (9 males and 15 females) have valid US

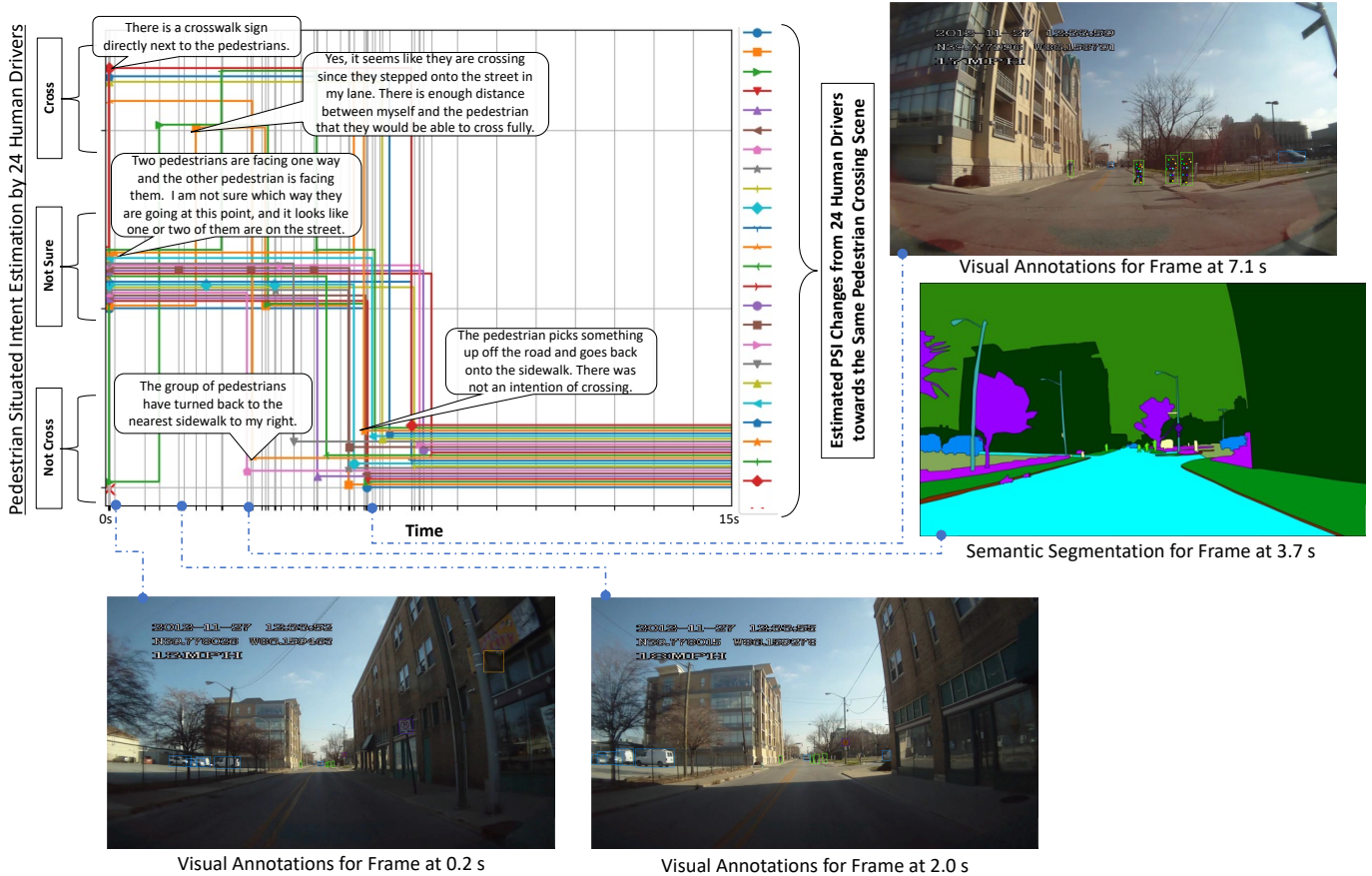


Fig. 1. Example of visual and cognitive annotations for a case that pedestrians did not cross in front of the ego-car eventually.

driving licenses, and are from 19 to 77 years old. The diverse backgrounds of annotators can ensure the representativeness of pedestrian intent estimation results and reasoning descriptions.

Cognitive Annotation Statistics: For all the 25,881 annotated video images, 24 annotators have estimated the Pedestrian Situated Intent frame by frame individually to achieve a total of more than 621k intent estimations. There are 5,473 Pedestrian Situated Intent segmentation boundaries in the entire data set across all the annotators and encounters. On average, each scene has 49.8 boundaries from all the annotators. Accordingly, there are 5,473 segments in all the intent segmentation curves with the same number of reasoning descriptions. Each encounter has 24 polygonal segmentation curves from all the subjects. On average, each annotator has 2.1 segments for each encounter case in estimating Pedestrian Situated Intent. The average length of the reasoning descriptions is 151.4 characters.

Annotation Discrepancies: Because each encounter is annotated by 24 video annotators with different backgrounds, there are similarities and discrepancies in intent estimation and reasoning descriptions. The similarities can reflect common sense and social norms, and individual differences mainly cause the discrepancies. The agreement score among annotators/drivers in pedestrian intent estimation is defined as the highest percentage of annotators who agree on the same pedestrian intent for a certain timestamp. In that case, we calculate the disagreement score as $1 - \text{agreement}$ for all the frames across all the cases. The results show two findings. **On**

the one hand, more than 95% of the encounter scenes has an average disagreement score of less than 20% across the whole duration, meaning that the annotators can achieve consensus in estimating Pedestrian Situated Intent in most situations. **On the other hand**, more than 70% of cases has a maximum disagreement score of more than 50%, meaning that there are certain moments in most cases that more than half of the annotators do not achieve the same Pedestrian Situated Intent estimations.

C. Annotation Process

Low-level Annotation Process. To obtain the ground-truth for low-level annotations, team members used Computer Vision Annotation Tool (CVAT) to manually annotate every frame in the dataset for bounding boxes, human pose estimation, and semantic segmentation while using the tracking feature. CVAT supports a range of annotation tasks, including but not limited to a rectangle, point, polygon, polyline, 3D, and attribute annotating. CVAT also supports semi-automatic and automatic labeling using pre-trained models along with support for multiple data annotation formats.

(i) **Object Detection.** Rectangular 2D bounding boxes are annotated to locate traffic objects and agents such as vehicles, traffic sign, building, vegetation, sky and so on. Each object is given a unique ID, and pedestrians are annotated with occlusion attributes.

(ii) **Posture.** Identified pedestrians are annotated with a maximum of 17 key points to create a pose estimation. Five

key points map the face, while the remaining 12 maps the pedestrian’s body. Each key point is associated with the pedestrian’s unique ID.

(iii). *Tracking*. Both bounding boxes and pose estimation are annotated with tracking features to allow for temporal processing.

(iv). *Semantic Segmentation*. Polygons are annotated on one key frame per video to classify each pixel in the image with a label.

Cognitive Annotation Process. In order to obtain the cognitive annotations, a video experiment was conducted for all the recruited 24 video annotators. Previous studies have used video experiments to study human neural and cognitive mechanisms in the activity segmentation process [40], investigate the driver’s decision-making process in predicting pedestrian’s behaviors [41], and explain the driving behaviors with text descriptions [17]. Furthermore, a recent study [11] adopted a similar video experiment process to annotate pedestrians’ desire to cross the street. In that study, a group of human drivers was recruited to watch pedestrian-encountering videos in the PIE dataset and label the estimated intent of the pedestrian to cross the street at the predetermined frame for each case. Please note that the intent defined in the PIE dataset [11] is static and is a higher-level plan compared with the Pedestrian Situated Intent in this study.

We extended the existing video experiments to obtain the desired cognitive annotations. Event-segmentation [42], [43] and predictive-processing [44] models are prevailing theories to explain human cognition during interactions, emphasizing the facts that human brains segment continued scene perceptions based on intention boundaries of others, code activities in each segment as events, and infer future intention boundaries based on event coherence [45]. In order to capture this cognitive process, one browser-based data annotation platform was developed to support the cognitive annotation process. All the 110 videos of pedestrian encountering scenes are presented to each of the 24 data annotators sequentially through the developed user interface. Each video will play and pause at the first frame when the pedestrian is visible, with the targeted pedestrian pointed out by a red arrow. Each annotator needs to estimate the pedestrian’s intent to cross in front of the ego-vehicle at that moment based on the preceding scenes. A brief reasoning description is provided to support such estimation.

After the first frame, the data annotator needs to estimate the Pedestrian Situated Intent frame by frame until the end of the video. If the pedestrian intent changes at a particular frame, one segmentation boundary is inserted, and a reasoning description is required to explain the situation. The results capture how the pedestrian’s intent to cross in front of the ego-vehicle changes along with the changes of the situations from the perspective of this annotator.

This annotation process was completed by all 24 annotators for all the 110 scenes. Although these intent annotations were not provided by the pedestrians in those situations directly, they reflect the estimation of Pedestrian Situated Intents during the interactions from the average driver’s perspective. In most cases, pedestrian intent is dynamic, non-deterministic,

and based upon the driver’s responses that are relying on the driver’s understanding of the scenes. This fact means that the driver’s estimated Pedestrian Situated Intents, rather than the actual intents directly collected from the pedestrian, determines how the car responds to the situations during the interactions with pedestrians and affects the actual pedestrian intents in return. Thus, we believe that these Pedestrian Situated Intent annotations from the drivers’ perspectives can serve as ground-truth estimations for the AI algorithms to learn and further guide the behavior planning for the automated cars during interactions with pedestrians.

III. THE PROPOSED ALGORITHM

The three tasks we perform on the PSI dataset are pedestrian intent prediction, pedestrian trajectory prediction, and driver reasoning explanation. The former two use the lower-level visual annotations to predict pedestrian intent aggregated from the cognitive annotations, as well as the pedestrian future bounding box positions. The latter tries to predict the human reasoning descriptions through visual scene understanding. Considering the strong relationship between intention and behaviors [12] and the prior findings of improved trajectory prediction with intention modules [11], [27], the Pedestrian Situated Intent is predicted in the eP2P algorithm to guide the crossing trajectory prediction directly. In addition, the human reasoning annotations capture background knowledge and can help refining the focus of the system to the more relevant cues, and the human annotation disagreement levels reflect the scene uncertainty for intent estimation. Both of these annotations will be modeled into the algorithm design to improve trajectory prediction with better modeling human scene understanding. Furthermore, when all these annotations are predicted explicitly, the algorithm can be better explained with multimodal outputs besides trajectory predictions.

To this end, we design our **eP2P** algorithm by estimating the conditional distribution $\mathbf{p}(\mathbf{L}_{traj}^\tau | \mathbf{V}_{cxt}^t, \mathbf{L}_{ped}^t, \mathbf{I}_{int}^t, \mathbf{R}_{rsn}^t, \mathbf{D}_{agr}^t)$ illustrated as Figure 2 and pipe-lined with five modules. $\mathbf{V}_{cxt} = \{\mathbf{v}^i\}_{i=t-m}^{t+\tau}$, $\mathbf{L}_{ped} = \{\mathbf{l}^i\}_{i=t-m}^{t+\tau}$, $\mathbf{I}_{int} = \{\mathbf{c}^i\}_{i=t-m}^{t+\tau}$, $\mathbf{R}_{rsn} = \{\mathbf{r}^i\}_{i=t-m}^{t+\tau}$, $\mathbf{D}_{agr} = \{\mathbf{d}^i\}_{i=t-m}^{t+\tau}$ are the sequence of global-visual context, pedestrian location, crossing intention, visual reasoning, and human disagreement from time $t-m$ to $t+\tau$, respectively. During training, all data in are accessible, while evaluating, only sequence within $[t-m, t]$ are observed, denoted as $\mathbf{V}_{cxt}^t, \mathbf{L}_{ped}^t, \mathbf{I}_{int}^t, \mathbf{R}_{rsn}^t, \mathbf{D}_{agr}^t$. The predicted pedestrian trajectory for the future τ time period is denoted as $\mathbf{L}_{traj}^\tau = \{\mathbf{l}^i\}_{i=t+1}^{t+\tau}$, where \mathbf{l} is the 2D bounding box of the pedestrian, defined by the top-left and bottom-right corner points $[(x_1, y_1), (x_2, y_2)]$.

Context Feature Extraction: In order to integrate the vital information encoded in the target pedestrian’s appearance (e.g., pose, motion, action, etc.) and surrounding environment (e.g., location, traffic signals, vehicles, etc.), we deploy a Convolutional-LSTM module to extract global-local context features. Specifically, the whole global frame and local regions cropped by the twice enlarged pedestrian bounding boxes are input to the convolutional backbone, then concatenated as input to the context feature extractor, whose last hidden state

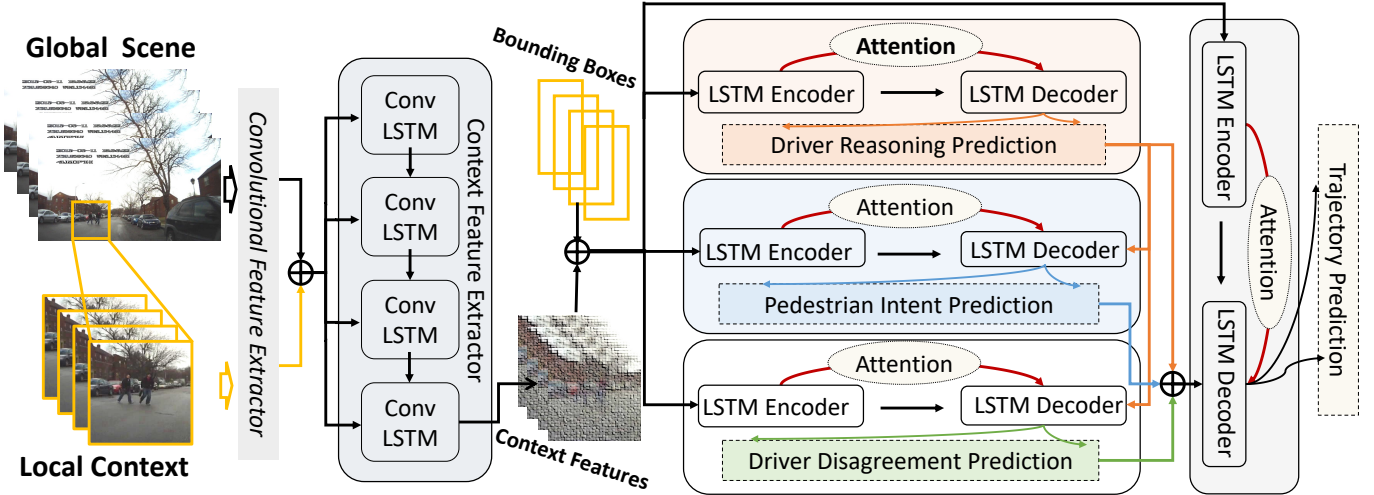


Fig. 2. Pipeline of our proposed framework, with inputs of $t - m \sim t$ past frames and outputs of $t + 1 \sim t + \tau$ future frames. The model consists of five modules from left to right: *Context Feature Extraction*, *Visual Reasoning Estimation*, *Pedestrian Intent Estimation*, *Human Disagreement Estimation*, and *Pedestrian Trajectory Prediction*.

plays the context features for the following reason, intention, disagreement, and pedestrian trajectory prediction.

Driver Reasoning/Disagreement and Pedestrian Intent Prediction: For predicting pedestrian intention annotations in the PSI dataset, we employ three LSTM encoder-decoder modules with attention mechanism to predict the future $t + 1 \sim t + \tau$ frames driver reasoning, Pedestrian Situated Intent, and driver disagreement, respectively. Specifically, the learned visual context features are concatenated with the target pedestrian bounding boxes coordinates as the input to the encoders in all three modules. For decoders, the predicted τ human reasoning is also input to the decoders predicting crossing intention and disagreement. Moreover, multi-layer perceptron attention layer [46] is adopted bridging the encoder and decoder to capture the most relevant information in the observed sequence. In addition, a self-attention layer is applied to the decoder inputs for the intention and disagreement estimation. The final predictions are generated by a linear projection of the decoder’s output. For reason prediction, binary cross-entropy loss is defined as:

$$\mathcal{L}_{rsn} = \frac{1}{N\tau} \sum_{i=1}^N \sum_{j=t+1}^{t+\tau} \text{BCE}(\mathbf{r}_i^j, \hat{\mathbf{r}}_i^j), \quad (1)$$

where $\hat{\mathbf{r}}_i^j$ is the predicted reason for frame i at time j . For intention estimation, cross-entropy loss is adopted as:

$$\mathcal{L}_{int} = \frac{1}{N\tau} \sum_{i=1}^N \sum_{j=t+1}^{t+\tau} \text{CE}(\mathbf{c}_i^j, \hat{\mathbf{c}}_i^j), \quad (2)$$

where $\hat{\mathbf{c}}_i^j$ is the predicted crossing intention. Prior works consider the target pedestrian is annotated with the same road-crossing desire for the whole pedestrian encountering duration [11], which actually is not directly related to crossing actions. We use the Pedestrian Situated Intent as a changing status to address this issue. For disagreement score prediction, mean squared error loss is adopted as:

$$\mathcal{L}_{agr} = \frac{1}{N\tau} \sum_{i=1}^N \sum_{j=t+1}^{t+\tau} \text{MSE}(\mathbf{d}_i^j, \hat{\mathbf{d}}_i^j), \quad (3)$$

where $\hat{\mathbf{d}}_i^j$ is the predicted disagreement score.

Trajectory Prediction: Eventually, we adopt an LSTM encoder-decoder module to predict the future τ frames’ pedestrian trajectory. All obtained predictions of driver reasoning, Pedestrian Situated Intent, and driver disagreements are concatenated and input to the decoder, and the context features concatenated with the bounding boxes are input to the encoder. The outputs of the decoder are input to a fully-connected layer to predict the target pedestrian’s future locations coordinates. The optimization objective is mean-square error loss as:

$$\mathcal{L}_{traj} = \frac{1}{N\tau} \sum_{i=1}^N \sum_{j=t+1}^{t+\tau} \text{MSE}(\mathbf{l}_i^j, \hat{\mathbf{l}}_i^j), \quad (4)$$

where $\hat{\mathbf{l}}_i^j$ is the predicted location from sample i at time j .

To sum up, we integrate all objectives to formulate our overall loss function for the proposed model as $\mathcal{L} = \mathcal{L}_{rsn} + \mathcal{L}_{int} + \mathcal{L}_{agr} + \mathcal{L}_{traj}$.

IV. EXPERIMENTS

A. Experimental Setup

Datasets. For all 110 videos in the PSI dataset, the first 75 videos are used for training, video 76 to 80 are adopted for validation, and the rest videos make up the test set. For all annotated frames, we sample clip of length 15 with overlap ratio as 0.8. For intention prediction, with input 15 observed frames, we predict the target pedestrian crossing intention at the 16-th frame. For trajectory prediction, with the observed 15-frame sequence, we predict the target pedestrian’s bounding box locations for the following 0.5s, 1.0s, and 1.5s.

To predict the intention of a pedestrian, we split each video clip into multiple sequences of length 15 frames using a sliding window. For the i -th observed sequence, $S_{obs}^i = \{s_0^i, s_1^i, \dots, s_{14}^i\}$, we predict the crossing intention, c^i , of the pedestrian. We define two sub-tasks for predicting intention. The first is a binary classification task with labels “crossing” and “not crossing” derived from aggregated intention annotations. We perform this first task on three algorithms on PSI. The second sub-task is a multi-class classification task with intention being three labels, “crossing”, “not crossing”,

and “unsure”. We perform this multi-class classification task on only two algorithms excluding the PIE model. We adopt classification accuracy and F1-score. The detailed process of human annotation is provided in supplemental material.

Evaluation metrics. For intention prediction, we report the overall accuracy, class-wise average accuracy, and the *macro* average F1 scores. For the trajectory prediction, we evaluate the model with Average Displacement Error ($ADE = \frac{1}{N \times \tau} \sum_{i=1}^N \sum_{j=t+1}^{t+\tau} \|\mathbf{I}_i^j - \hat{\mathbf{I}}_i^j\|_2$), Final Displacement Error ($FDE = \frac{1}{N \times \tau} \sum_{i=1}^N \|\mathbf{I}_i^{t+\tau} - \hat{\mathbf{I}}_i^{t+\tau}\|_2$), which are measured based on the center coordinates of the pedestrian bounding boxes. In addition, average and final RMSE of bounding boxes coordinates are also reported as ARB and FRB, respectively, following [47], [48], [28], [49]. All trajectory prediction metrics are reported in pixel level for 0.5s, 1.0s, and 1.5s prediction lengths.

Implementation details. We accept ResNet-50 [50] pre-trained on ImageNet [51] without the last fully-connected layer as the convolutional feature extractor. The context feature extractor includes one-layer convolutional LSTM with 64 filters and kernel size of 2×2 with stride 1 for encoder, and one-layer LSTM with 64 hidden units as decoder. For the reasoning prediction, we use LSTM encoder-decoder framework with 128 hidden units. For intention/disagreement/trajectory prediction, we use LSTM encoder-decoder with 64 hidden units, and self-attention layer is applied to the decoder inputs, and a multi-layer perceptron attention layer [46] connects the encoder and decoder hidden states. Dropout is set as 0.5 for all layers. The model is trained by Adam optimizer with learning rate initialized as $l_0 = 1e^{-3}$, annealing as $l_p = \frac{l_0}{(1+\delta p)^q}$, where p is the progress of training epochs linearly changing from 0 to 1, $\delta = 10$, $q = 0.75$, and the max number of epochs is 1,000 with early-stop strategy applied to stop training based on the performance on validation set. The source code is available <https://github.com/PSI-Intention2022/PSI-Intention>.

B. Results of Three Tasks on PSI

Task 1. Pedestrian Situated Intent Prediction

Two pedestrian intention prediction baseline models are compared with ours. The first is taken from the intention prediction module of PIE [11]. PIE uses expanded visual information around the pedestrian and pedestrian bounding box location with an LSTM encoder-decoder to predict crossing intention. The second baseline is VR-GCN from [52] which uses the visual features of all relevant traffic agents and objects to create a spatio-temporal graph for reasoning with additional features from bounding box location and pose estimation. Similar to PIE, VR-GCN [52] uses an LSTM encoder-decoder to predict the intention. Experimental results for pedestrian intent prediction are reported in Table II.

For the multi-class classification task towards three states of pedestrian intents, our model achieves an accuracy of 0.58 and the F1 score of 0.53. The baseline results suggest that the temporal-dynamic PSI labels are more challenging to predict, especially when the “Not Sure” label is considered. This particular “Not Sure” label represents the most challenging

interaction phases, which are even difficult for human drivers to estimate or achieve consensus. However, these challenging phases are highly non-deterministic and critical for vehicle-pedestrian negotiations in a natural road environment. Thus, more advanced pedestrian intent prediction models need to be developed and trained.

In the binary-classification task, we try to compare the performance of other two baseline algorithms [11], [52] on the PSI. As summarized in Table II, our model can still reach good accuracy (0.76), the balanced accuracy (0.67) and F1 score (0.66), and all the metrics for the PIE algorithm (accuracy of 0.69, balanced accuracy of 0.58, and F1 score of 0.79) drop significantly when predicting the situated intent on PSI dataset. This result again highlights that the PSI dataset provides more realistic and also more challenging situations. Some demo prediction results are illustrated in Figure 3, showing correct and incorrect prediction outputs from three algorithms. The PSI label is temporal-dynamic and contingent on the situations, which can be quite straightforward or much more challenging to learn in different segments. The current experiment does not consider more advanced algorithm structure and training strategies, and thus does not adapt to the realistic interactions very well in some circumstances.

Task 2. Reasoning Explanation Prediction

Our intention prediction module is applied to predict the pedestrian crossing or not, and semantic explanation. Figure 4 shows selected samples of both crossing intention and explanation prediction generated by our model. For crossing-intention prediction, “G” denotes the ground-truth, and “P” is the predicted result. For explanation, green ones are the correctly predicted sentences, red ones are wrong prediction, and the gray ones are in the ground-truth explanations but not predicted correctly.

One annotation video demo is also provided. The video clip shows the visual annotations, situated intent segmentation results from all 24 human annotators, and some selected explanations for one of the 110 annotated cases. The bottom-left part of the video demo shows the aggregated pedestrian situated intent across all the 24 human annotators. Then the binary prediction results from the two baseline algorithms for PSI are also illustrated.

Task 3. Pedestrian Trajectory Prediction

We compare the results of our proposed model with two baselines for the pedestrian trajectory prediction on PSI dataset as shown in Table III. Specifically, $LSTM_{ed}^{bbox}$ is the LSTM encoder-decoder with only pedestrian bounding boxes as input, and PIE_{traj} is the PIE model with local context around the pedestrian as input. From the results we observe that our model outperforms the compared baselines on all tasks. It is noteworthy that, our proposed model can provide prediction explanation and disagreement prediction in addition to the pedestrian intention and trajectory prediction, which is incapable for other baselines.

V. CONCLUSION

In this paper, we introduced the IUPUI-CSRC Pedestrian Situated Intent (PSI) dataset. The dataset has been released

TABLE II
COMPARISON OF PREDICTION RESULTS FOR DIFFERENT BASELINE MODELS ON TWO BENCHMARK DATASETS FOR PREDICTING PEDESTRIAN INTENTS.

Datasets	Baseline	Accuracy	Balanced Accuracy	F1-Score
PSI (3 class)	VR-GCN [52]	0.53	0.59	0.48
	Ours	0.58	0.55	0.53
PSI (binary)	VR-GCN [52]	0.74	0.61	0.64
	PIE [11]	0.69	0.58	0.79
	Ours	0.76	0.67	0.66

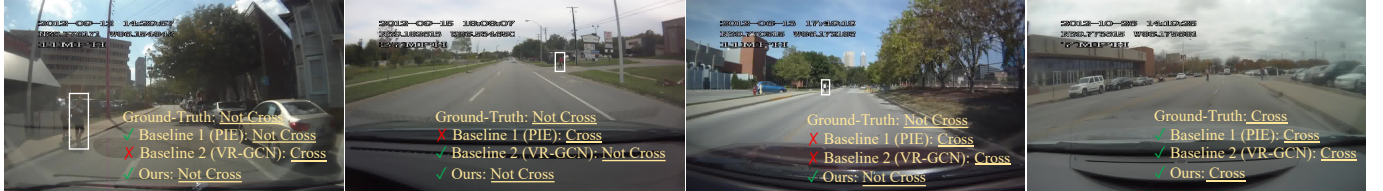


Fig. 3. Binary intent prediction results from the three methods in comparison with the ground-truth aggregated across 24 annotators for PSI.



Fig. 4. Visualization of pedestrian intent and explanation prediction on PSI.

and available to the public to access. The **PSI** dataset has the most comprehensive visual annotations, and more importantly, highlights two novel cognitive annotations in the domains of pedestrian behavior prediction and autonomous driving. The first one is the temporal-dynamic pedestrian intent to cross in front of the ego-vehicle during vehicle-pedestrian interactions. The second one is the explanations of human reasoning synchronized with estimating such pedestrian intents in different situations. Compared with all the existing benchmark datasets, both of these cognitive labels are original and can fundamentally improve the current designs of pedestrian behavior prediction and driving decision-making algorithms towards socially intelligent AVs. To demonstrate the use of **PSI** dataset in predicting pedestrian intents and human explanations, we developed an explainable Pedestrian Trajectory Prediction (**eP2P**) model and evaluated on multiple tasks.

REFERENCES

- [1] A. M. Boggs, B. Wali, and A. J. Khattak, "Exploratory analysis of automated vehicle crashes in california: A text analytics & hierarchical bayesian heterogeneity-based approach," *Accident Analysis & Prevention*, vol. 135, p. 105354, 2020.
- [2] J. E. Domeyer, J. D. Lee, and H. Toyoda, "Vehicle automation—other road user communication and coordination: Theory and mechanisms," *IEEE Access*, vol. 8, pp. 19 860–19 872, 2020.
- [3] K. Li, S. Eiffert, M. Shan, F. Gomez-Donoso, S. Worrall, and E. Nebot, "Attentional-gcn: Adaptive pedestrian trajectory prediction towards generic autonomous vehicle use cases," in *2021 IEEE International Conference on Robotics and Automation (ICRA)*. IEEE, 2021, pp. 14 241–14 247.
- [4] H. Chen and X. Zhang, "Path planning for intelligent vehicle collision avoidance of dynamic pedestrian using att-lstm, msfm and mpc at un-signalized crosswalk," *IEEE Transactions on Industrial Electronics*, 2021.
- [5] W. Wu, H. Jia, Q. Luo, and Z. Wang, "Dynamic path planning for autonomous driving on branch streets with crossing pedestrian avoidance guidance," *IEEE Access*, vol. 7, pp. 144 720–144 731, 2019.

TABLE III
COMPARISON OF PREDICTION RESULTS FOR DIFFERENT BASELINE MODELS ON PSI DATASETS FOR PREDICTING PEDESTRIAN TRAJECTORY.

	0.5s				1.0s				1.5s			
	ADE↓	FDE↓	ARB↓	FRB↓	ADE↓	FDE↓	ARB↓	FRB↓	ADE↓	FDE↓	ARB↓	FRB↓
LSTM _{ed} ^{bbbox}	27.51	37.34	31.05	40.31	39.87	66.56	43.07	69.34	55.47	105.9	58.51	108.62
PIE _{traj}	23.63	32.73	29.89	34.59	35.39	61.50	37.45	63.40	52.18	101.9	54.27	103.46
Ours	22.67	27.73	27.12	31.59	31.07	52.03	35.03	55.08	44.90	93.14	48.51	95.97

- [6] A. Best, S. Narang, D. Barber, and D. Manocha, "Autonovi: Autonomous vehicle planning with dynamic maneuvers and traffic constraints," in *2017 IEEE/RSJ International Conference on Intelligent Robots and Systems (IROS)*. IEEE, 2017, pp. 2629–2636.
- [7] T. Chen and R. Tian, "A survey on deep-learning methods for pedestrian behavior prediction from the egocentric view," in *2021 IEEE International Intelligent Transportation Systems Conference (ITSC)*. IEEE, 2021, pp. 1898–1905.
- [8] E. Vinkhuyzen and M. Cefkin, "Developing socially acceptable autonomous vehicles," in *Ethnographic Praxis in Industry Conference Proceedings*, vol. 2016, no. 1. Wiley Online Library, 2016, pp. 522–534.
- [9] H. R. Pelikan, "Why autonomous driving is so hard: The social dimension of traffic," in *Companion of the 2021 ACM/IEEE International Conference on Human-Robot Interaction*, 2021, pp. 81–85.
- [10] S. Zhang, M. Abdel-Aty, Y. Wu, and O. Zheng, "Pedestrian crossing intention prediction at red-light using pose estimation," *IEEE Transactions on Intelligent Transportation Systems*, 2021.
- [11] A. Rasouli, I. Kotseruba, T. Kunic, and J. K. Tsotsos, "Pie: A large-scale dataset and models for pedestrian intention estimation and trajectory prediction," in *Proceedings of the IEEE/CVF International Conference on Computer Vision*, 2019, pp. 6262–6271.
- [12] I. Ajzen, "The theory of planned behavior," *Organizational behavior and human decision processes*, vol. 50, no. 2, pp. 179–211, 1991.
- [13] D. Dey and J. Terken, "Pedestrian interaction with vehicles: roles of explicit and implicit communication," in *Proceedings of the 9th international conference on automotive user interfaces and interactive vehicular applications*, 2017, pp. 109–113.
- [14] M. Sucha, D. Dostal, and R. Rissler, "Pedestrian-driver communication and decision strategies at marked crossings," *Accident Analysis & Prevention*, vol. 102, pp. 41–50, 2017.
- [15] R. M. Hogarth, T. Lejarraja, and E. Soyer, "The two settings of kind and wicked learning environments," *Current Directions in Psychological Science*, vol. 24, no. 5, pp. 379–385, 2015.
- [16] É. Zablocki, H. Ben-Younes, P. Pérez, and M. Cord, "Explainability of vision-based autonomous driving systems: Review and challenges," *arXiv preprint arXiv:2101.05307*, 2021.
- [17] J. Kim, A. Rohrbach, T. Darrell, J. Canny, and Z. Akata, "Textual explanations for self-driving vehicles," in *Proceedings of the European conference on computer vision (ECCV)*, 2018, pp. 563–578.
- [18] A. Rasouli, I. Kotseruba, and J. K. Tsotsos, "Understanding pedestrian behavior in complex traffic scenes," *IEEE Transactions on Intelligent Vehicles*, vol. 3, no. 1, pp. 61–70, 2017.
- [19] M. F. Elahi, J. G. Sreeram, X. Luo, and R. Tian, "A novel adaptation of information extraction algorithm to process natural text descriptions of pedestrian encounters," in *2021 IEEE International Intelligent Transportation Systems Conference (ITSC)*. IEEE, 2021, pp. 1906–1912.
- [20] Z. Hou, X. Peng, Y. Qiao, and D. Tao, "Visual compositional learning for human-object interaction detection," in *European Conference on Computer Vision*. Springer, 2020, pp. 584–600.
- [21] K. Kato, Y. Li, and A. Gupta, "Compositional learning for human object interaction," in *Proceedings of the European Conference on Computer Vision (ECCV)*, 2018, pp. 234–251.
- [22] M. A. Elliott, C. J. Armitage, and C. J. Baughan, "Drivers' compliance with speed limits: an application of the theory of planned behavior," *Journal of Applied Psychology*, vol. 88, no. 5, p. 964, 2003.
- [23] G. Sukthankar, C. Geib, H. H. Bui, D. Pynadath, and R. P. Goldman, *Plan, activity, and intent recognition: Theory and practice*. Newnes, 2014.
- [24] G. Markkula, R. Madigan, D. Nathanael, E. Portouli, Y. M. Lee, A. Dietrich, J. Billington, A. Schieben, and N. Merat, "Defining interactions: A conceptual framework for understanding interactive behaviour in human and automated road traffic," *Theoretical Issues in Ergonomics Science*, vol. 21, no. 6, pp. 728–752, 2020.
- [25] L. A. Suchman, *Plans and situated actions: The problem of human-machine communication*. Cambridge university press, 1987.
- [26] I. Kotseruba, A. Rasouli, and J. K. Tsotsos, "Joint attention in autonomous driving (jaad)," *arXiv preprint arXiv:1609.04741*, 2016.
- [27] B. Liu, E. Adeli, Z. Cao, K.-H. Lee, A. Shenoi, A. Gaidon, and J. C. Nibbles, "Spatiotemporal relationship reasoning for pedestrian intent prediction," *IEEE Robotics and Automation Letters*, vol. 5, no. 2, pp. 3485–3492, 2020.
- [28] S. Malla, B. Dariush, and C. Choi, "Titan: Future forecast using action priors," in *Proceedings of the IEEE/CVF Conference on Computer Vision and Pattern Recognition*, 2020, pp. 11 186–11 196.
- [29] W. Kim, M. S. Ramanagopal, C. Barto, M.-Y. Yu, K. Rosaen, N. Goumas, R. Vasudevan, and M. Johnson-Roberson, "Pedx: Benchmark dataset for metric 3-d pose estimation of pedestrians in complex urban intersections," *IEEE Robotics and Automation Letters*, vol. 4, no. 2, pp. 1940–1947, 2019.
- [30] F. Yu, W. Xian, Y. Chen, F. Liu, M. Liao, V. Madhavan, and T. Darrell, "Bdd100k: A diverse driving video database with scalable annotation tooling," *arXiv preprint arXiv:1805.04687*, vol. 2, no. 5, p. 6, 2018.
- [31] X. Huang, P. Wang, X. Cheng, D. Zhou, Q. Geng, and R. Yang, "The apolloscope open dataset for autonomous driving and its application," *IEEE transactions on pattern analysis and machine intelligence*, vol. 42, no. 10, pp. 2702–2719, 2019.
- [32] H. Caesar, V. Bankiti, A. H. Lang, S. Vora, V. E. Liong, Q. Xu, A. Krishnan, Y. Pan, G. Baldan, and O. Beijbom, "nusences: A multimodal dataset for autonomous driving," in *Proceedings of the IEEE/CVF conference on computer vision and pattern recognition*, 2020, pp. 11 621–11 631.
- [33] J. Geyer, Y. Kassahun, M. Mahmudi, X. Ricou, R. Durgesh, A. S. Chung, L. Hauswald, V. H. Pham, M. Mühlegg, S. Dorn *et al.*, "A2d2: Audi autonomous driving dataset," *arXiv preprint arXiv:2004.06320*, 2020.
- [34] M.-F. Chang, J. Lambert, P. Sangkloy, J. Singh, S. Bak, A. Hartnett, D. Wang, P. Carr, S. Lucey, D. Ramanan *et al.*, "Argoverse: 3d tracking and forecasting with rich maps," in *Proceedings of the IEEE/CVF Conference on Computer Vision and Pattern Recognition*, 2019, pp. 8748–8757.
- [35] S. Ettinger, S. Cheng, B. Caine, C. Liu, H. Zhao, S. Pradhan, Y. Chai, B. Sapp, C. Qi, Y. Zhou *et al.*, "Large scale interactive motion forecasting for autonomous driving: The waymo open motion dataset," *arXiv preprint arXiv:2104.10133*, 2021.
- [36] R. Tian, L. Li, K. Yang, S. Chien, Y. Chen, and R. Sherony, "Estimation of the vehicle-pedestrian encounter/conflict risk on the road based on taxi 110-car naturalistic driving data collection," in *2014 IEEE Intelligent Vehicles Symposium Proceedings*. IEEE, 2014, pp. 623–629.
- [37] H. Xu, Y. Gao, F. Yu, and T. Darrell, "End-to-end learning of driving models from large-scale video datasets," in *Proceedings of the IEEE conference on computer vision and pattern recognition*, 2017, pp. 2174–2182.
- [38] Y. Xu, X. Yang, L. Gong, H.-C. Lin, T.-Y. Wu, Y. Li, and N. Vasconcelos, "Explainable object-induced action decision for autonomous vehicles," in *Proceedings of the IEEE/CVF Conference on Computer Vision and Pattern Recognition*, 2020, pp. 9523–9532.
- [39] T.-Y. Lin, M. Maire, S. Belongie, J. Hays, P. Perona, D. Ramanan, P. Dollár, and C. L. Zitnick, "Microsoft coco: Common objects in context," in *European conference on computer vision*. Springer, 2014, pp. 740–755.
- [40] J. Q. Sargent, J. M. Zacks, D. Z. Hambrick, R. T. Zacks, C. A. Kurby, H. R. Bailey, M. L. Eisenberg, and T. M. Beck, "Event segmentation ability uniquely predicts event memory," *Cognition*, vol. 129, no. 2, pp. 241–255, 2013.
- [41] S. Schmidt and B. Faerber, "Pedestrians at the kerb—recognising the action intentions of humans," *Transportation research part F: traffic psychology and behaviour*, vol. 12, no. 4, pp. 300–310, 2009.

- [42] J. M. Zacks and K. M. Swallow, "Event segmentation," *Current directions in psychological science*, vol. 16, no. 2, pp. 80–84, 2007.
- [43] C. A. Kurby and J. M. Zacks, "Segmentation in the perception and memory of events," *Trends in cognitive sciences*, vol. 12, no. 2, pp. 72–79, 2008.
- [44] J. Hohwy, A. Hebblewhite, and T. Drummond, "Events, event prediction, and predictive processing," *Topics in cognitive science*, vol. 13, no. 1, pp. 252–255, 2021.
- [45] D. A. Baldwin and J. E. Kosie, "How does the mind render streaming experience as events?" *Topics in Cognitive Science*, vol. 13, no. 1, pp. 79–105, 2021.
- [46] D. Bahdanau, K. Cho, and Y. Bengio, "Neural machine translation by jointly learning to align and translate," *arXiv preprint arXiv:1409.0473*, 2014.
- [47] A. Gupta, J. Johnson, L. Fei-Fei, S. Savarese, and A. Alahi, "Social gan: Socially acceptable trajectories with generative adversarial networks," in *Proceedings of the IEEE conference on computer vision and pattern recognition*, 2018, pp. 2255–2264.
- [48] A. Rasouli, M. Rohani, and J. Luo, "Bifold and semantic reasoning for pedestrian behavior prediction," in *Proceedings of the IEEE/CVF International Conference on Computer Vision*, 2021, pp. 15 600–15 610.
- [49] J. Liang, L. Jiang, J. C. Niebles, A. G. Hauptmann, and L. Fei-Fei, "Peeking into the future: Predicting future person activities and locations in videos," in *Proceedings of the IEEE/CVF Conference on Computer Vision and Pattern Recognition*, 2019, pp. 5725–5734.
- [50] K. He, X. Zhang, S. Ren, and J. Sun, "Deep residual learning for image recognition," in *Proceedings of the IEEE conference on computer vision and pattern recognition*, 2016, pp. 770–778.
- [51] J. Deng, W. Dong, R. Socher, L.-J. Li, K. Li, and L. Fei-Fei, "Imagenet: A large-scale hierarchical image database," in *2009 IEEE conference on computer vision and pattern recognition*. Ieee, 2009, pp. 248–255.
- [52] T. Chen, R. Tian, and Z. Ding, "Visual reasoning using graph convolutional networks for predicting pedestrian crossing intention," in *Proceedings of the IEEE/CVF International Conference on Computer Vision*, 2021, pp. 3103–3109.